Supporting Information

Layered Ion Dynamics and Enhanced Energy Storage: VS_2/MXene Heterostructure Anodes Revolutionizing Li-Ion Batteries

*Mahendiraprabu Ganesan[a] and Jin Yong Lee[a]**

Department of Chemistry, Sungkyunkwan University, Suwon 16419, Korea

Fig. S1. Optimized structures of the (a) $VS_2/Ti_3C_2O_2$ and (b) $VS_2/V_3C_2O_2$ heterostructures were obtained through concentration variations with Li-loading.

Fig. S2. The charge density (a - d) and charge density difference (e - h) plots for $VS_2/Ti_3C_2O_2$ heterostructures with Li-loading. The symbols "+" and "-" indicates electron accumulation and depletion regions respectively.

Fig. S3. The charge density (a - d) and charge density difference (e - h) plots for $VS_2/V_3C_2O_2$ heterostructures with Li-loading. The symbols "+" and "-" indicates electron accumulation and depletion regions respectively.

Fig. S4. The projected band structures with corresponding total density of states for $VS_2/Ti_3C_2O_2$ heterostructures with Li-loading.

Fig. S5. The projected band structures with corresponding total density of states for $VS_2/V_3C_2O_2$ heterostructures with Li-loading.

Fig. S6. The AIMD simulations for $VS_2/Ti_3C_2O_2$ heterostructures with Li-loading at 300K.

Fig. S7. The AIMD simulations for $VS_2/V_3C_2O_2$ heterostructures with Li-loading at 300K.

Fig. S8. The AIMD simulations for Variation of interlayer spacing Vs time steps (fs) of $VS_2/Ti_3C_2O_2$ heterostructures with Li-loading.

Fig. S9. The AIMD simulations for Variation of interlayer spacing Vs time steps (fs) of $VS_2/V_3C_2O_2$ heterostructures with Li-loading.

Table S1 Calculated lattice parameters (a=b), thicknesses, M–C bond lengths (d_{M-C}, M = Ti or V), M–O bond lengths (d_{M-O}, M = Ti or V), V–S bond lengths (d_{V-S}) and O–S bond lengths (d_{O-S}) in the monolayer and $VS_2/M_3C_2O_2$ hetrostructures. All distances are in Å units.

Table S2 The interlayer distances (E_{int} in Å) for Li ions adsorbed between $VS_2/M_3C_2O_2$ heterostructures.

Table S3 The adsorption energy (E_{ad} in eV) for Li ions adsorbed between $VS_2/M_3C_2O_2$ heterostructures.

Table S4 The open circuit voltages (OCV in V) for Li ions in $VS_2/M_3C_2O_2$ heterostructures.

Table S5 The storage capacities (q in $mAhg^{-1}$) of $VS_2/M_3C_2O_2$ heterostructures.

Table S6 Comparison of the Performance of Current Work with Previously Reported 2D Material-Based Li-Ion Batteries.

Table S7 The average bond distances (in Å) for Li ions adsorbed between $VS_2/M_3C_2O_2$ heterostructures.

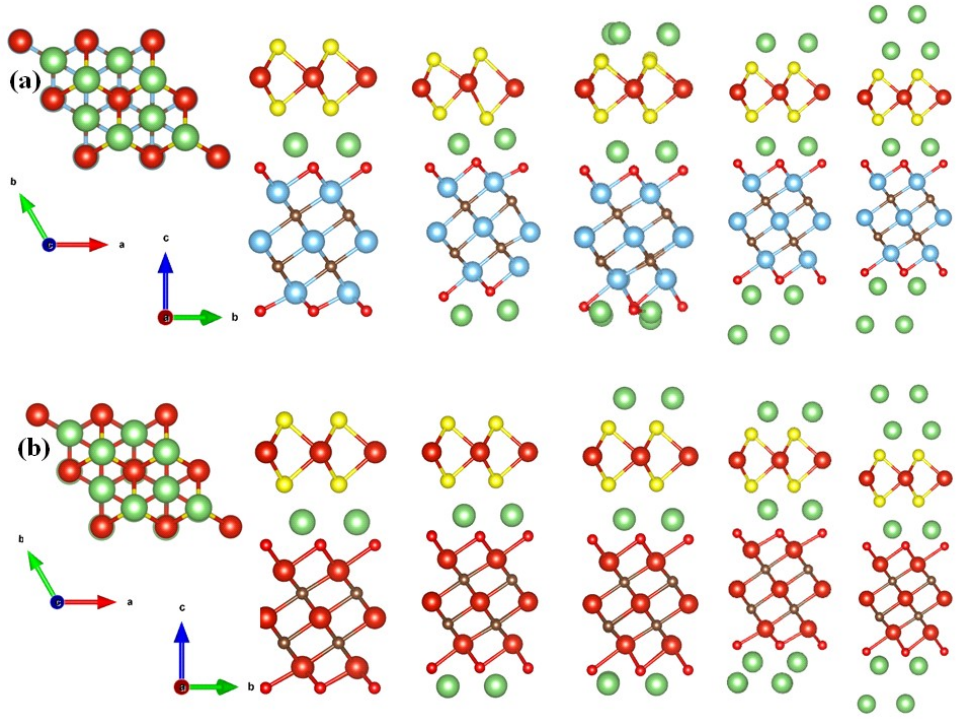

Fig. S1. Optimized structures of the (a) $VS_2/Ti_3C_2O_2$ and (b) $VS_2/V_3C_2O_2$ heterostructures were obtained through concentration variations with Li-loading.

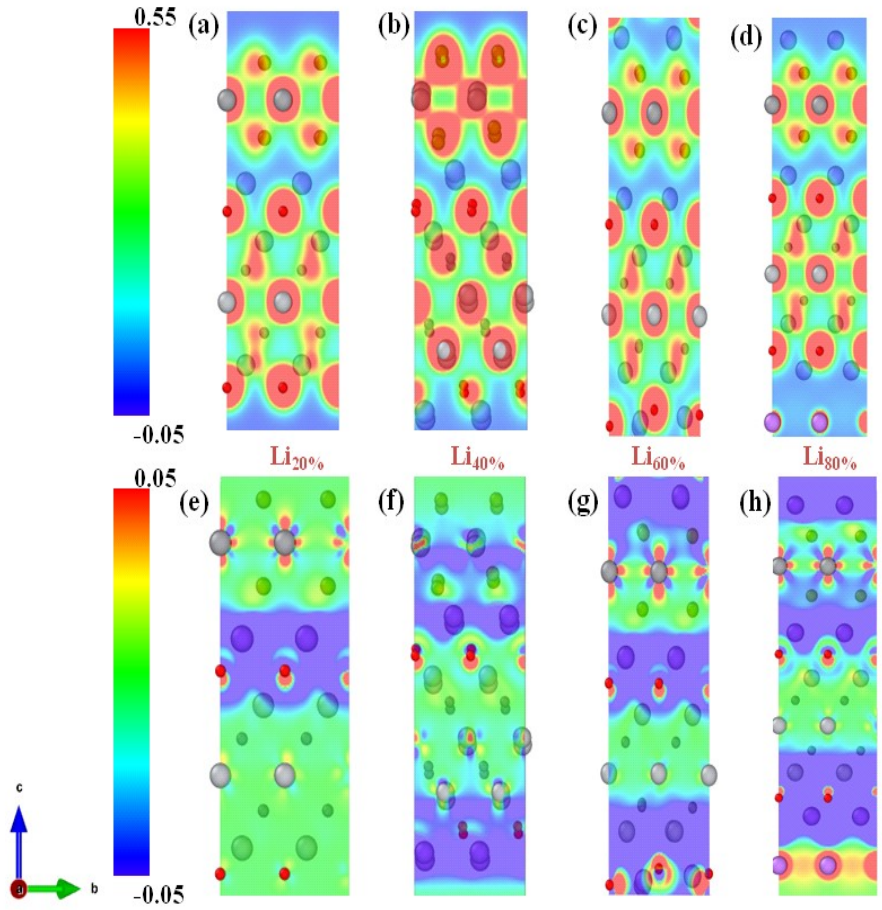

Fig. S2. The charge density (a - d) and charge density difference (e - h) plots for $VS_2/Ti_3C_2O_2$ heterostructures with Li-loading. The symbols "+" and "-" indicates electron accumulation and depletion regions respectively.

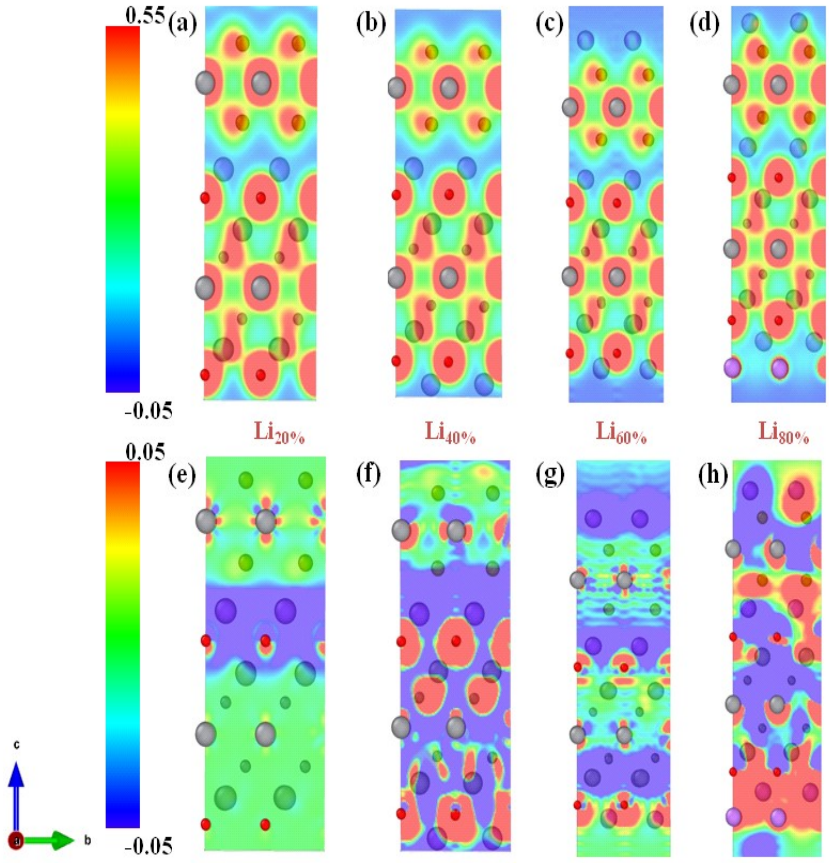

Fig. S3. The charge density (a - d) and charge density difference (e - h) plots for $VS_2/V_3C_2O_2$ heterostructures with Li-loading. The symbols "+" and "-" indicates electron accumulation and depletion regions respectively.

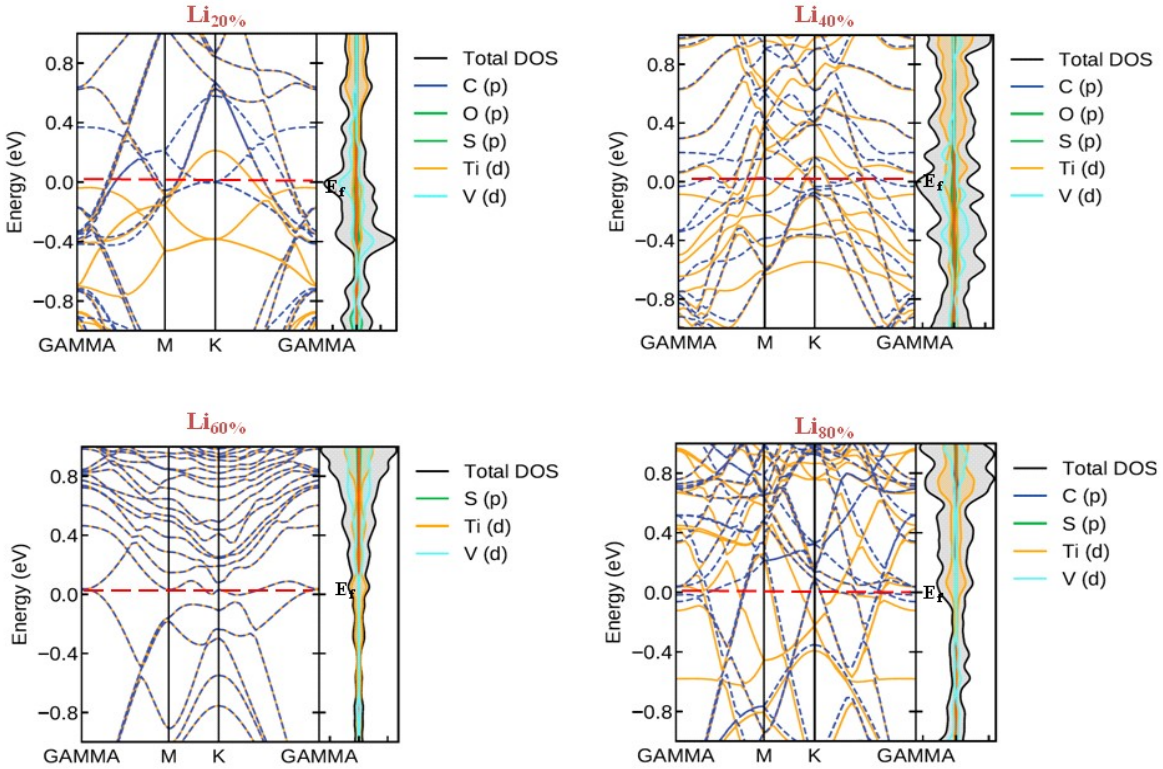

Fig. S4. The projected band structures with corresponding total density of states for $VS_2/Ti_3C_2O_2$ heterostructures with Li-loading.

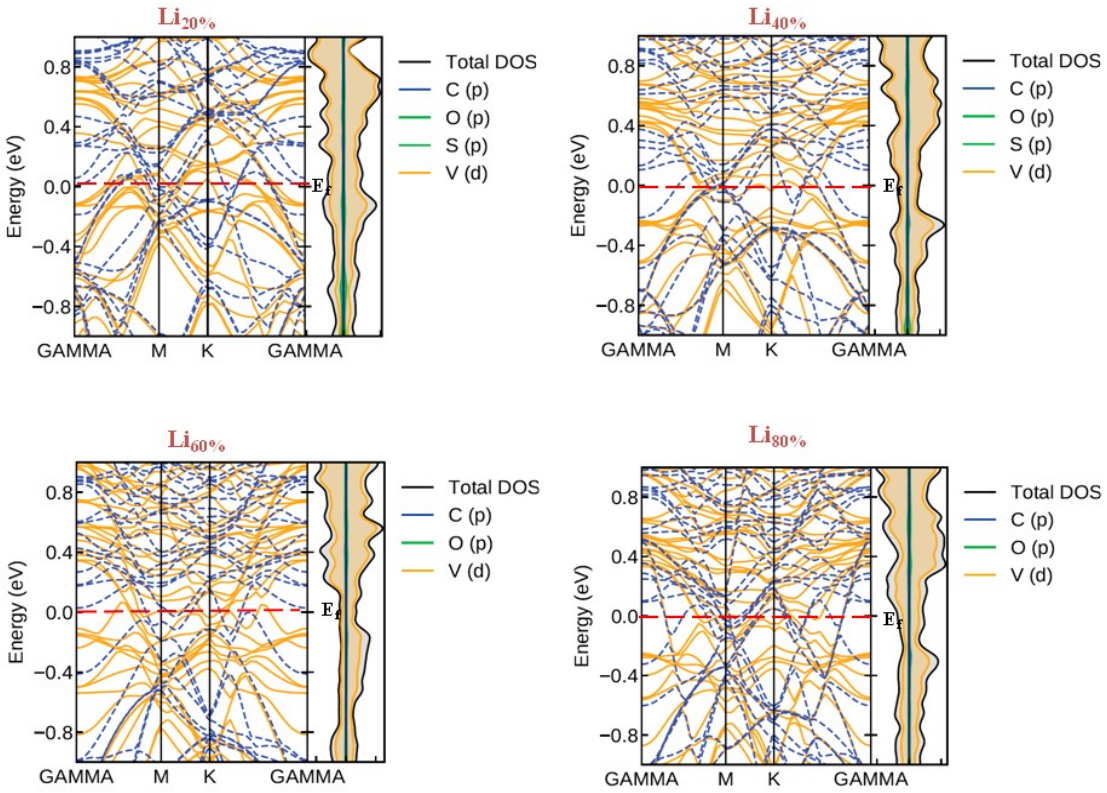

Fig. S5. The projected band structures with corresponding total density of states for $VS_2/V_3C_2O_2$ heterostructures with Li-loading.

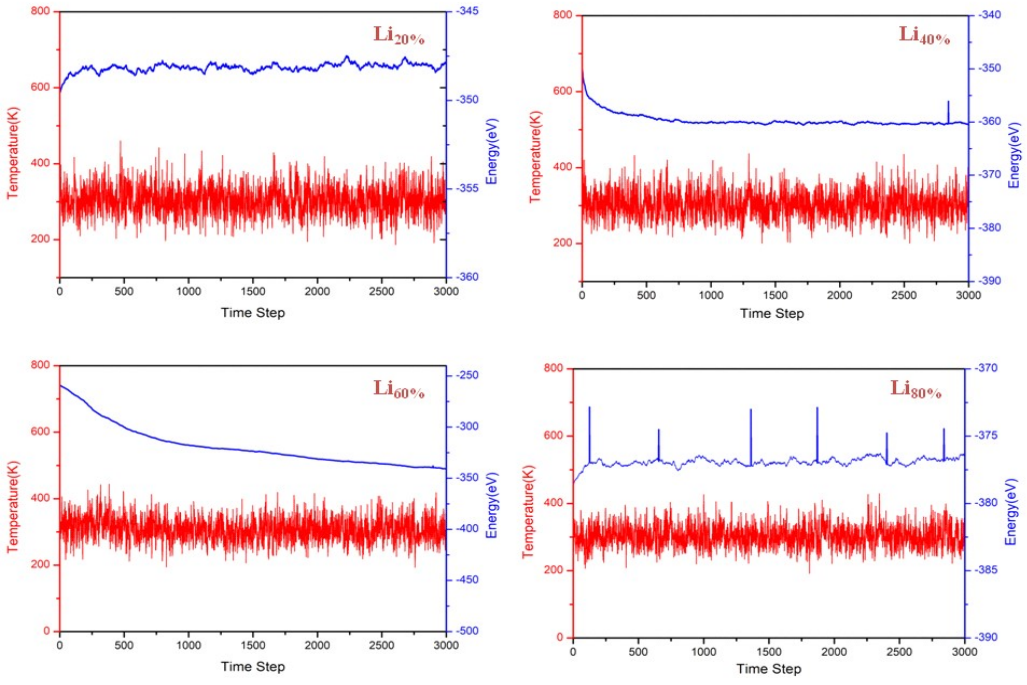

Fig. S6. The AIMD simulations for $VS_2/Ti_3C_2O_2$ heterostructures with Li-loading at 300K.

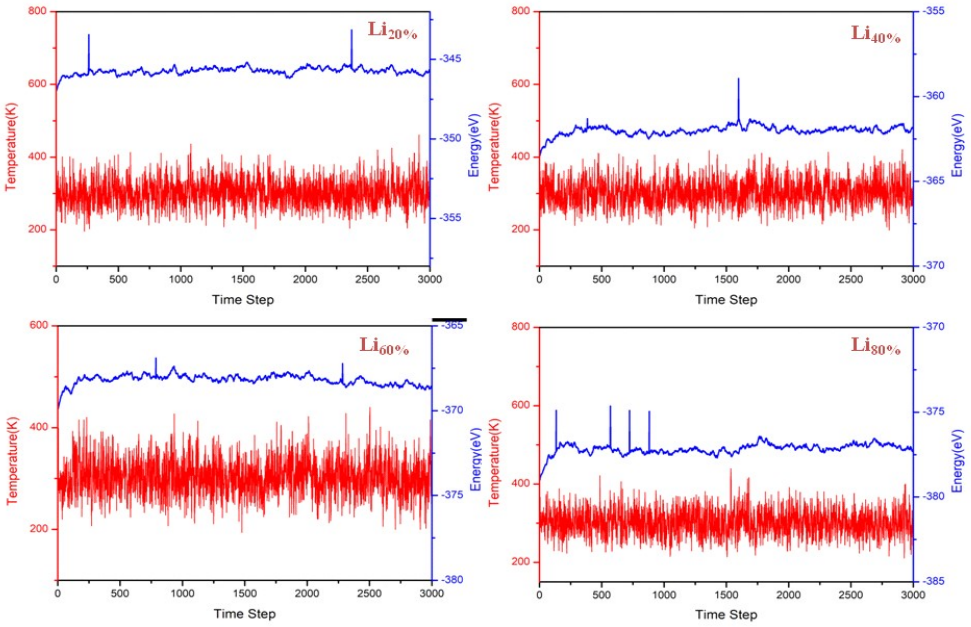

Fig. S7. The AIMD simulations for $VS_2/V_3C_2O_2$ heterostructures with Li-loading at 300K.

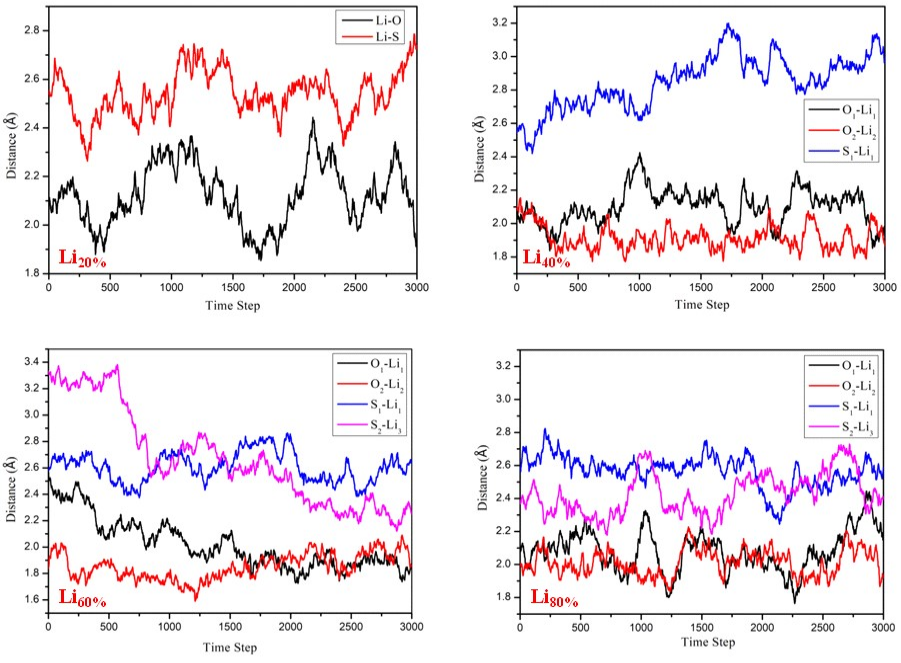

Fig. S8. The AIMD simulations for Variation of interlayer spacing Vs time steps (fs) of $VS_2/Ti_3C_2O_2$ heterostructures with Li-loading.

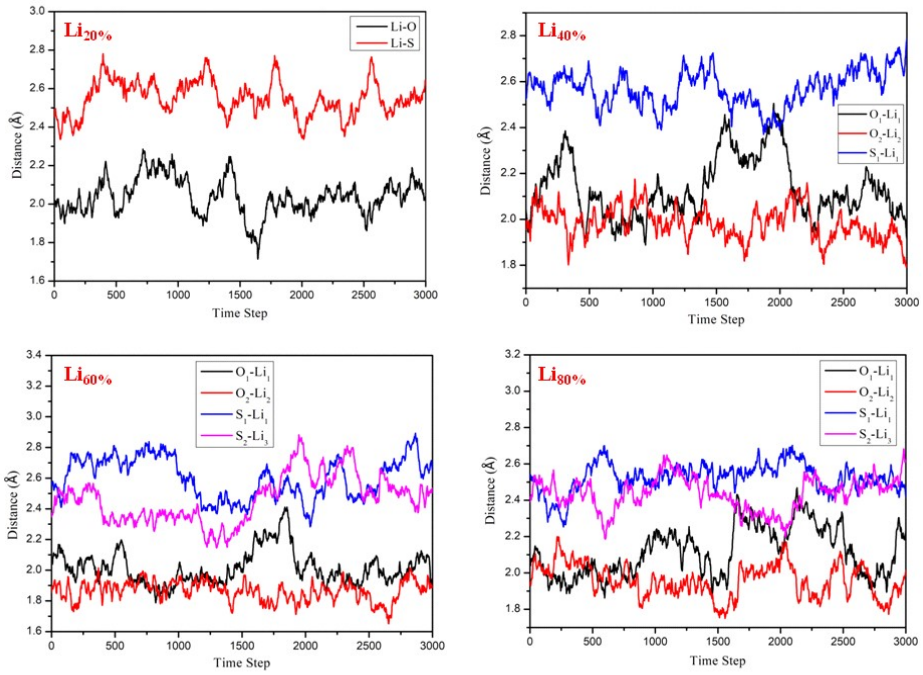

Fig. S9. The AIMD simulations for Variation of interlayer spacing Vs time steps (in fs) of $VS_2/V_3C_2O_2$ heterostructures with Li-loading.

Table S1 Calculated lattice parameters (a=b), thicknesses, M–C bond lengths (d_{M-C}, M = Ti or V), M–O bond lengths (d_{M-O}, M = Ti or V), V–S bond lengths (d_{V-S}) and O–S bond lengths (d_{O-S}) in the monolayer and $VS_2/M_3C_2O_2$ hetrostructures. All distances are in Å units.

Materials	a=b	Thickness	d_{M-C}	d_{M-O}	d_{V-S}	d_{O-S}
$Ti_3C_2O_2$	5.89	6.96	2.18	1.97	---	---
$V_3C_2O_2$	5.80	6.81	2.06	1.95	---	---
VS_2	6.33	2.99	---	---	2.36	---
$VS_2/Ti_3C_2O_2$	6.11	12.86	2.19	1.98	2.33	3.32
$VS_2/V_3C_2O_2$	5.92	12.73	2.07	1.98	2.31	3.29

Table S2 The interlayer distances (E_{int} in Å) for Li ions adsorbed between $VS_2/M_3C_2O_2$ heterostructures.

$VS_2/Ti_3C_2O_2$	d_{O1-S1}	d_{O1-Li1}	d_{Li1-S1}	d_{C1-Li1}	d_{C2-Li2}	d_{C1-Li3}	d_{O2-Li4}	d_{S2-Li5}
Pure	3.32	---	---	---	---	---	---	---
$Li_{20\%}$	3.45	2.09	2.54	3.50	---	---	---	---
$Li_{40\%}$	3.45	2.09	2.54	3.50	3.52	---	---	---
$Li_{60\%}$	3.45	2.05	2.63	3.37	2.72	9.81	---	---
$Li_{80\%}$	3.45	2.07	2.58	3.44	3.34	9.92	4.59	---
$Li_{100\%}$	3.45	2.09	2.55	3.47	3.34	9.92	4.64	4.06
$VS_2/V_3C_2O_2$								
Pure	3.29	---	---	---	---	---	---	---
$Li_{20\%}$	3.34	2.03	2.47	3.37	---	---	---	---
$Li_{40\%}$	3.42	2.05	2.52	3.42	3.30	---	---	---
$Li_{60\%}$	3.45	2.04	2.57	3.41	3.14	9.95	---	---
$Li_{80\%}$	3.45	2.03	2.53	3.49	3.19	10.00	4.55	---
$Li_{100\%}$	3.45	2.04	2.54	3.43	3.25	10.00	4.58	4.07

Table S3 The adsorption energy (E_{ad} in eV) for Li ions adsorbed between $VS_2/M_3C_2O_2$ heterostructures.

Li content	$VS_2/Ti_3C_2O_2$	$VS_2/V_3C_2O_2$
$Li_{20\%}$	-2.86	-2.65
$Li_{40\%}$	-2.76	-2.49
$Li_{60\%}$	-1.55	-1.58
$Li_{80\%}$	-1.13	-1.29
$Li_{100\%}$	-1.01	-0.96

Table S4 The open circuit voltages (OCV in V) for Li ions in $VS_2/M_3C_2O_2$ heterostructures.

Li content	$VS_2/Ti_3C_2O_2$	$VS_2/V_3C_2O_2$
$Li_{20\%}$	3.14	2.60
$Li_{40\%}$	2.18	1.67
$Li_{60\%}$	1.27	0.75
$Li_{80\%}$	1.23	0.74
$Li_{100\%}$	1.30	0.73

Table S5 The storage capacities (q in $mAhg^{-1}$) of $VS_2/M_3C_2O_2$ heterostructures.

Li content	$VS_2/Ti_3C_2O_2$	$VS_2/V_3C_2O_2$
$Li_{20\%}$	85.17	82.64
$Li_{40\%}$	170.34	165.28
$Li_{60\%}$	255.50	247.91
$Li_{80\%}$	340.67	330.55
$Li_{100\%}$	425.84	413.19

Table S6 Comparison of the Performance of Current Work with Previously Reported 2D Material-Based Li-ion Batteries.

Material Structure	Reported Capacity ($mAhg^{-1}$)	References
Ti_3C_2	447.8	[Ref][1]
V_3C_2	606.42	[Ref] [2]
VS_2	195.4	[Ref] [3]
V_3C_2/graphene	598.63	[Ref] [4]
$V_2O_5/Ti_3C_2T_X$	321	[Ref] [5]
VS_2/Ti_2CO_2	462.08	[Ref] [6]
Ti_2CO_2/graphene	426	[Ref] [7]
$MoS_2/Ti_3C_2T_X$	153	[Ref][8]
$VS_2/Ti_3C_2O_2$	425.84	Current Work
$VS_2/V_3C_2O_2$	413.19	Current Work

Table S7 The average bond distances (in Å) for Li ions adsorbed between $VS_2/M_3C_2O_2$ heterostructures.

Concentration	$VS_2/Ti_3C_2O_2$				$VS_2/V_3C_2O_2$			
	$d_{O1\text{-}Li1}$	$d_{O2\text{-}Li2}$	$d_{S1\text{-}Li1}$	$d_{S2\text{-}Li3}$	$d_{O1\text{-}Li1}$	$d_{O2\text{-}Li2}$	$d_{S1\text{-}Li1}$	$d_{S2\text{-}Li3}$
$Li_{20\%}$	2.12	---	2.54	---	2.04	---	2.55	---
$Li_{40\%}$	2.10	1.92	2.85	---	2.13	1.98	2.57	---
$Li_{60\%}$	2.02	1.85	2.61	2.67	2.01	1.86	2.60	2.46
$Li_{80\%}$	2.08	2.01	2.57	2.43	2.11	1.96	2.53	2.44
$Li_{100\%}$	2.15	2.00	2.65	2.37	2.05	2.02	2.64	2.47

References

1 D. Er, J. Li, M. Naguib, Y. Gogotsi en V. B. Shenoy, *ACS Appl. Mater. Interfaces*, 2014, 6, 11173–11179.

2 K. Fan, Y. Ying, X. Li, X. Luo en H. Huang, *J. Phys. Chem. C*, 2019, 123, 18207–18214.

3 J. Z. Liu en P. F. Guo, *Wuji Cailiao Xuebao/Journal Inorg. Mater.*, 2015, 30, 1339–1344.

4 P. P. Dinda en S. Meena, J. *Phys: Condens. Matter*., 2021, 33, 175001 .

5 Y. Wang, T. Lubbers, R. Xia, Y.-Z. Zhang, M. Mehrali, M. Huijben en J. E. ten Elshof, *J. Electrochem. Soc.*, 2021, 168, 020507.

6 D. X. Song, L. Xie, Y. F. Zhang, Y. Lu, M. An, W. G. Ma en X. Zhang, *ACS Appl. Energy Mater.*, 2020, 3, 7699–7709.

7 Y. T. Du, X. Kan, F. Yang, L. Y. Gan en U. Schwingenschlögl, *ACS Appl. Mater. Interfaces*, 2018, 10, 32867–32873.

8 D. Wang, Y. Gao, Y. Liu, Y. Gogotsi, X. Meng, G. Chen en Y. Wei, *J. Mater. Chem. A*, 2017, 5, 24720–24727.